Progress In Electromagnetics Research, Vol. 125, 1–19, 2012

SIGNAL PROPAGATION ANALYSIS FOR LOW DATA RATE WIRELESS SENSOR NETWORK APPLICATIONS IN SPORT GROUNDS AND ON ROADS

D. L. Ndzi[1, *], M. A. M. Arif[2], A. Y. M. Shakaff[2], M. N. Ahmad[2], A. Harun[2], L. M. Kamarudin[3], A. Zakaria[2], M. F. Ramli[2], and M. S. Razalli[3]

[1]School of Engineering, University of Portsmouth, Portsmouth, PO1 3DJ, UK

[2]School of Mechatronic Engineering, University of Malaysia Perlis, Perlis, Malaysia

[3]School of Computer and Communication Engineering, University of Malaysia Perlis, Perlis, Malaysia

Abstract—This paper presents results of a study to characterise wireless point-to-point channel for wireless sensor networks applications in sport hard court arenas, grass fields and on roads. Antenna height and orientation effects on coverage are also studied and results show that for omni-directional patch antenna, node range is reduced by a factor of 2 when the antenna orientation is changed from vertical to horizontal. The maximum range for a wireless node on a hard court sport arena has been determined to be 70 m for 0 dBm transmission but this reduces to 60 m on a road surface and to 50 m on a grass field. For horizontal antenna orientation the range on the road is longer than on the sport court which shows that scattered signal components from the rougher road surface combine to extend the communication range. The channels investigated showed that packet error ratio (PER) is dominated by large-scale, rather than small-scale, channel fading with an abrupt transition from low PER to 100% PER. Results also show that large-scale received signal power can be modeled with a 2nd order log-distance polynomial equation on the sport court and road, but a 1st order model is sufficient for the grass field. Small-scale signal variations have been found to have a Rice distribution for signal to noise ratio levels greater than 10 dB but the Rice K-factor exhibits

Received 14 November 2011, Accepted 13 January 2012, Scheduled 14 February 2012

* Corresponding author: David L. Ndzi (David.Ndzi@port.ac.uk).

significant variations at short distances which can be attributed to the influence of strong ground reflections.

1. INTRODUCTION

Wireless sensor network (WSN) devices are envisioned to be widely used to monitor many systems thereby facilitating automation. Significant research efforts have been devoted towards improving WSN architectures, accuracy, efficiency and operations [1–5]. Many new applications have also emerged [6–11]. The development of the standards for short range wireless communication has made the implementation of WSN systems, co-existence with other wireless devices and, interoperability, much easier than before. However achieving optimum performance and minimizing cost in a wide area WSN deployment is still a major challenge [12].

Optimal propagation is an important requirement in wireless communication in order to maintain connectivity and a good quality of service. Channel measurements are often augmented with modeling and simulations to provide a wider assessment of system performances for different configurations in different scenarios [13–15]. Studies of wireless signal propagation to assess WSN performance in indoor and outdoor environments revealed that multipath fading significantly affects the accuracy of WSN applications such as in localization [16–18]. In [19] measurements and analyses of PER in WSN showed that 10% of the data is lost at a range of 7 m and 100% at 30 m. In that study the nodes were placed on the floor which blocked the first Fresnel zone. In most WSN network performance analysis, the two ray channel model [20] is often used. This, however, under represents the complexity of the propagation channel. The low transmission power characteristic of WSN devices means that most of the envisaged applications are in areas where line of sight (LOS) path between the transmitter and receiver exist [21].

Some of the applications of WSN are in buildings to monitor their structural integrity [22, 23]. They can also be used on roads to monitor road surfaces, monitor and control traffic [24, 25] and, for vehicle to vehicle and vehicle to curb (roadside) communications. Applications in sport are also expected to grow owing to the falling cost, reducing size and improvements in battery technology. In [26] WSN has been used to monitor the performance of rowers on boats and compare performances amongst team members. Dhamdhere et al. [27] have also implemented WSN to monitor football players and transmit real-time information to the sideline. However the emphasis was on routing and their results showed that the time delay to deliver information from players to the

sideline was unacceptably long due to the multi-hop routing technique used. This problem could have been ameliorated with an efficient single hop or direct transmission.

In road transport, cameras are widely used to provide information on road and traffic conditions. This often requires an operator to relay information to motorists and, hence, it is prone to human error. In addition, weather conditions such as fog or poor lighting could compromise the accuracy of the information. The deployment of sensors to monitor car speeds, road surfaces, tunnels [28], etc. and even, types of vehicles, can provide real-time accurate information. In [29] an adaptive segmentation method for traffic flow time-series analysis and in-network aggregation algorithm for data fusion for real-time traffic management is presented. In [30] a WSN system is proposed for vehicle to vehicle and vehicle to central command centre for traffic congestion management and to detect speeding vehicles. These systems either rely on multi-hop routing to transmit information from origin to destination or they make assumptions about the potential range of each node. In [32] an implementation that assumes the average transmission range of each node to be between 500 m and 1 km is described. The focus of most studies has been on the system architecture [31] and little attention has been paid to wireless signal propagation issues. Research reported in [33] showed that vehicles induce signal fades that are up to 40 dB, even when they do not traverse the transmitter to receiver path.

In most implementations, since the communication channel is not accurately modeled, researchers circumvent network coverage problems by using a dense network of nodes and/or rely on multi-hop routing for information delivery [22, 28]. This is not only inefficient but increases the cost of deployment and maintenance. This paper reports on a study conducted in a sport arena, road and grass field to gain a better understanding of ad-hoc wireless sensor network signal propagation. The results reported in this paper have applications in a large number of areas ranging from personal wireless sensor devices for athletes to applications in road transport for road surface monitoring, curb to vehicle and vehicle to vehicle communications. The results show that surface roughness plays a critical role in wireless network coverage and antenna height is more critical than antenna orientation. This paper proposes a 2nd order log-distance path loss model for wireless sensor network planning for antenna heights from 0.5 m on the road and on hard surface sport grounds.

This paper is organized as follows; Section 2 describes the system that has been used to conduct experimental measurements, the measurement locations and the set-ups. Section 3 presents large-scale

(a) (b) (c)

Figure 1. WSN node, (a) PICDEMZ (motherboard and MRF24J40MA transceiver module), (b) MRF24J40MA transceiver module and (c) antenna physical characteristic and dimension.

signal variations with distance for the different scenarios and packet error ratio results. This is followed in Section 4 by the analysis and modeling of the large-scale and small-scale signal power variations. Conclusions are drawn in Section 5.

2. EXPERIMENTAL SYSTEM AND SETUP

Figure 1(a) shows a set of Microchip Technology Incorporation WSN node (model: PICDEMZ). It consists of a motherboard and a MRF24J40MA transceiver module. PICDEMZ contains a microprocessor and connects to the MRF24J40MA transceiver module, shown in Figure 1(b), which implements the IEEE 802.15.4 standard. The transceiver operates in the 2.405–2.48 GHz frequency band. The RF receiver sensitivity is rated at −94 dBm [34], however measurements by the authors showed that the receiver sensitivity is −90 dBm. The MRF24J40MA transceiver's micro-strip omni-directional antenna has an E-shape as shown in Figure 1(c) [21, 34].

Measurements were carried out in the following areas: an outdoor multi-purpose sports court, a wide tarred road which is also used to park large buses, and on a grass field. A photograph of the multi-purpose sports arena is shown in Figure 2(a). The surface is flat, hard and made of bituminous asphalt, typically used on hard tennis courts. The objective of the studies on the three surfaces was to enable the development of radio wave propagation channel models for WSN applications in sport arenas, smart road surfaces, building structure monitoring, and application in other environments with these types of surfaces.

During the measurements, one of the nodes (receiver) was connected to a laptop computer and it remained in a fixed position for

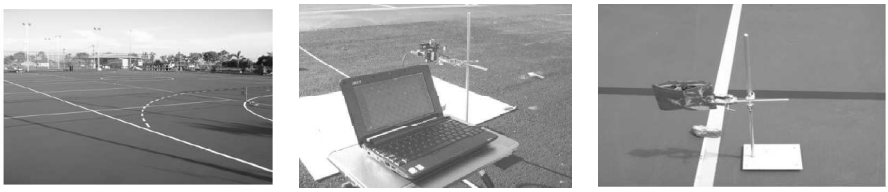

(a) (b) (c)

Figure 2. (a) Outdoor multipurpose sports arena, (b) receiver and (c) transmitter in the sports arena.

(a) (b) (c)

Figure 3. Test positions of WSN node, (a) vertical position, (b) horizontal position and (c) low position (0.09 m).

the duration of the measurements, as shown in Figure 2(b). It received transmitted packets and also measured the signal power levels.

The second WSN node (transmitter), shown in Figure 2(c), was placed at specific distances from the base station. It transmitted data packets 22 bytes long of Medium Access Control frames at a transmission power level of 0 dBm every 30 milliseconds. More than 1000 packets were transmitted and received at each location.

Four antenna settings were used for measurements on the court, 3 settings on the road and 2 on the grass field. These consisted of 2 antenna heights of 0.09 m (henceforth referred to as ground level) and 0.5 m, and 2 antenna orientations (vertical and horizontal). Figure 3 illustrates the antenna settings used. On the court, measurements were conducted with all the settings, on the road they were conducted at both heights but only with the vertical orientation at 0.09 m antenna height and; on the grass field measurements were carried out at both heights with only the vertical antenna orientation. They were repeated at different distances up to 50 m, depending on the signal strength and the ability of the nodes to still communicate.

From the antenna's data sheet, when it is vertically orientated it has the best radiation pattern. Relatively lower power is radiated in the intended direction when the antenna is in the horizontal position. However, the use of this type of antennas on sensor nodes,

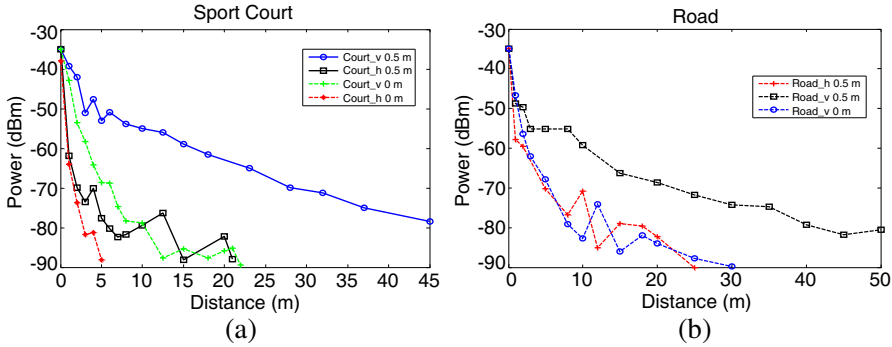

Figure 4. Comparison of signal power variation with distance at two antenna heights and orientation on (a) sport court and (b) road.

which may not always benefit from a fixed orientation due to ad-hoc node placements requires a careful assessment of the communication impairment and range restriction that the network may suffer due to antenna disorientation. Thus this study also aims to establish the limits (worst and best) of the system's performance in the selected environments.

3. MEASUREMENT RESULTS

Figure 4 shows a comparison between signal power variations with distance on the sport court and on the road. Antenna height gain at 0.5 m and correct patch antenna orientation increases the wireless node range by more than a factor of 2. Horizontal antenna orientation at 0.5 m height gives a similar range as vertical orientation at ground level in sport court. Vertical antenna orientation at ground level range is greater than horizontal antenna orientation at 0.5 m height by 5 m on the road as shown in Figure 4(b). Figure 4(a) also shows that for horizontal orientation at ground level the range is limited to 5 m.

Figure 5 compares the signal power variation at 0.5 m antenna heights on the court, road and grass field. Figure 5(a) shows that path loss is smaller on the sport court compared to on the road and grass. The sport court surface was smoother than the road and grass. Interestingly, for horizontal antenna orientation, signal attenuation over the court was higher compared to the road. The rougher road surface scatters the signal rather than the plane specula reflection that would be expected from the smoother court surface. The scattered signal enhances the signal strength and helps to extend the transmission range on the road.

From the number of received packets, the PER was computed

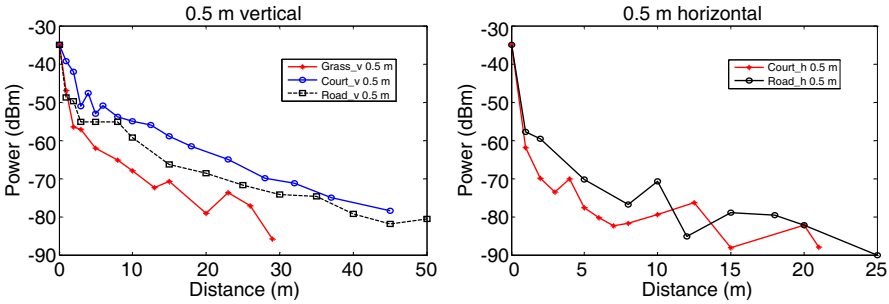

Figure 5. Comparison of signal variation at the same height over different surfaces for (a) vertical and (b) horizontal antenna orientations.

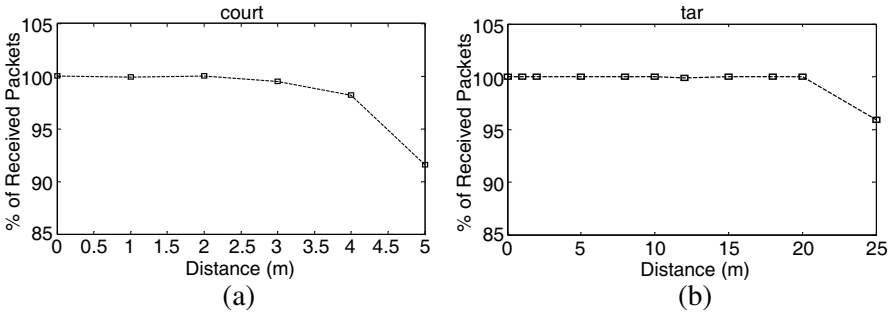

Figure 6. Percentage of received packets with distance for horizontal antenna (a) at ground level on sport court, and (b) 0.5 m height along the road.

for every continuous 1000 packets transmitted using Equation (1), as a percentage. This was carried out at each position. For reliable point to point communication, the PER percentage must be less than 1% [35, 36].

$$\text{PER} = \frac{(N_t - N_r)}{N_t} \times 100\% \tag{1}$$

where PER is in percentage, N_r is the number of received packets and N_t is the number of transmitted packets.

Figure 6 shows the percentage of received packets (packet delivery ratio) for horizontal antenna orientation on the sport court and on the road. Beyond the distances shown in the figures packet loss was 100% (PER of 100%). At the maximum range, the received signal power was close to or at the limit of the node sensitivity of −90 dBm. Of specific interest is the rate of packet loss which has been found not to be gradual

with range but abrupt for step distances of 4 m and above. This can be attributed to poor signal to noise ratio and the fact that the channels investigated were dominated by large scale path loss such that when it reached the limits, enhancements due to small-scale variations were not sufficient for any packets to be successfully received. ZigBee (IEEE 802.15.4) shares the 2.4 GHz band with WLAN (IEEE 802.11b/g), except for Zigbee's channels 25 and 26 that lie just outside the WLAN spectral mask. Although there were no WLAN transmissions within range during the measurements, such transmission will interfere with Zigbee and result in worse PER performance. Analysis of the impact of noise and co-interference between Zigbee and WLAN are presented in [37, 38]. Results of PER in [38] from an outdoor channel also show large transitions with distance. Results from the study reported in this paper show that a 20% margin of the maximum range would be required to ensure that PER is maintained within 2%. Due to the ad-hoc nature of most WSN deployments, the electromagnetic noise level and co-system interference must be taken into account when establishing this margin for any environment.

4. MEASUREMENT ANALYSIS AND RESULTS

4.1. Path Loss

Path loss models which are used to estimate signal variation with distance include Friis, Two Ray and log-distance models [18, 20]. Path loss model are generally regarded as large-scale models that can be used to predict average signal variations over large distances due to spatial separation between the transmitter and the receiver. They are important for network planning. However, at each distance the signal also exhibits temporal and spatial variations often referred to as small-scale fading. Knowledge of small-scale variations, especially at low signal to noise ratios, is critical for the assessment of the performances of coding and modulation schemes and, protocols.

For short range communication, the received signal can be modeled using Equation (2).

$$P_{r(\mathrm{dB})}(d) = P_{0(\mathrm{dB})} - 10 * n * \log_{10}(d) + p(x) \tag{2}$$

where $P_{r(\mathrm{dB})}$ is the received power, $P_{0(\mathrm{dB})}$ is the reference signal power which can be normalized to a reference distance, d is the distance between the transmitter and receiver antennas, n is the rate at which power decays with distance [10], and $p(x)$ is a zero-mean random variable that describes small-scale signal variation at each position along the propagation path. This equation assumes a homogeneous medium where the rate of signal attenuation is constant. If $n = 2$,

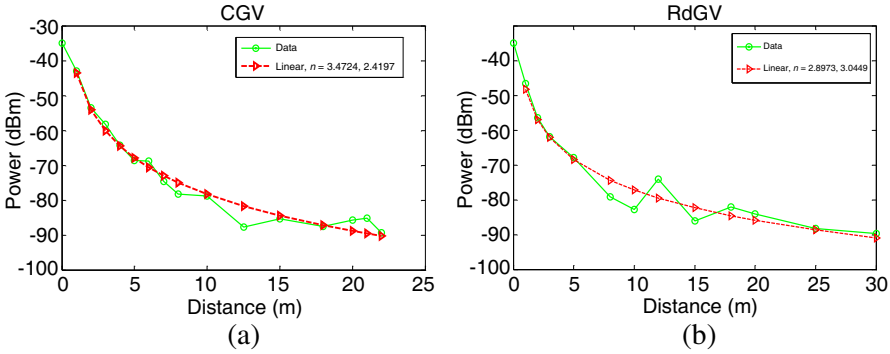

Figure 7. Model fitting to large scale signal variations for ground level antenna height on (a) sport court and (b) road.

this will be equivalent to normalized free space model. Signal power variation with distance, as shown in Figures 4 and 5 is large-scale variation (average power at each location) that can be modeled using Equation (2). Figure 7 shows examples of model fitting to signal variation.

As an example, Equation (3) is the model that describes large scale path loss in Figure 7(a). $P_{0(\mathrm{dB})}$ is effectively the received power at 1 m distance at which the curve has been normalized. The distribution $p(x)$, has not yet been determined.

$$P_{r(\mathrm{dB})}(d) = -43.59 - 34.72\log_{10}(d) + p(x) \tag{3}$$

The values of n and $P_{0(\mathrm{dB})}$, together with the root mean square (RMS) errors for all the measurements are given in Table 1 for first order linear model fittings. For antenna height of 0.5 m, n is close to 2, indicating that large-scale variation is close to free space value. The main exception is on the sport court where the rate of signal decays is less than that of free space. The smoothness of the court surface means that contributions from ground reflection were expected to be strong compared to the other surfaces.

Based on the first order model fittings for which the parameter values are presented in Table 1, the range of the wireless nodes for measurements at 0.5 m vertical antenna orientation in the sport court and on the road would exceed 100 m at −90 dBm signal level. This was believed to be too optimistic. A second order polynomial was then used to evaluate the signal variation. The improvements in RMS errors were minimal for all cases except for 0.5 m antenna height in the sport court and on the road. The RMS error for the 0.5 m antenna height on the court improved by 1 dB to 2.04 dB, and reduced to 1.57 dB for 0.5 m measurement on the road. For these two cases, the large-scale models

Table 1. Fitted parameter values and root mean square error.

Location	Antenna Orientation	Antenna Height (m)	Exponent n	P_0 (dB)	RMS Error
sport court	Vertical	0.09	3.47	−43.59	2.42
	Horizontal	0.09	3.28	−64.13	1.57
	Vertical	0.5	2.27	−35.64	3.04
	Horizontal	0.5	1.70	−64.19	3.35
Road	Vertical	0.5	2.07	−43.24	3.23
	Horizontal	0.5	2.15	−55.58	3.58
	Vertical	0.09	2.90	−48.20	3.04
Grass Field	Vertical	0.5	2.24	−46.97	2.64
	Vertical	0.09	3.11	−46.41	1.34

are represented by:

$$P_{rc(\mathrm{dB})}(d) = -10(\log_{10}(d))^2 - 4.961\log_{10}(d) - 41.89 + p(x) \quad (4)$$

$$P_{rr(\mathrm{dB})}(d) = -11.63(\log_{10}(d))^2 + 0.6\log_{10}(d) - 49.43 + p(x) \quad (5)$$

where $P_{rc(\mathrm{dB})}$ and $P_{rr(\mathrm{dB})}$ are the path loss models for the sport court and road, respectively for 0.5 m vertical antenna orientation. There is currently no clear physical explanation for this model, however the conjecture is that it is as a result of the complex interaction of multiple scattered and ground reflected signal components.

4.2. Small-scale Fading

A number of probability distributions can be used to describe small-scale signal fading, some of which have strong correlations with the prevailing propagation mechanisms, e.g., Rayleigh, Rice and Lognormal probability distributions. Other distributions act as intermediaries linking two distributions at each extremes, e.g., Nakagami with Rayleigh and Rice distributions as extremes, and Weibull distribution which interpolates between exponential distribution and Rayleigh distributions with shape parameter values of 1 and 2, respectively. These, and other probability distributions, have been used to evaluate the small-scale signal fading. Chi-square and Kolmogorov-Smirnov (K-S) goodness-of-fit tests have been used as criteria for selecting the best distribution [39, 40]. Chi-square (X^2) is described by Equation (6). When $X^2 = 0$, it indicates that the measured data is an absolute perfect fit to the model. For $X^2 > 0$, Chi Square table can be used to determine whether it exceeds the critical value for a chosen probability level, p, ($p = 0.05$ is widely used) to

reject the null hypothesis of equal distributions. The main limitation of the Chi-square goodness-of-fit test is that it depends on an adequate sample size for the approximations to be valid [41].

$$X^2 = \sum_{i=1}^{k} \frac{(f_i - P[x_i])^2}{P[x_i]} \tag{6}$$

where k is the number of intervals, i is the interval and f_i is the frequency of the measured data with the unit of number of the occurrence. $P[x_i]$ is the expected frequency of the data in the ith bin. The K-S test is an exact test that uses the empirical distribution function to measure the maximum distance between two curves (PDF and data in this case) and does not depend on the underlying distribution function being tested. The K-S test is defined by Equation (7).

$$D = \lim_{1 \le i \le N} \left(F(x_i) - \frac{i-1}{N}, \frac{i}{N} - F(x_i) \right) \tag{7}$$

where $F[x_i]$ is the theoretical cumulative distribution of the probability distribution being tested, i is the ith data point and N is the total number of data points. The main limitation of the K-S test is that the distribution must be continuous and fully specified.

Rice distribution often describes line-of-sight (LOS) signal variation [33]. For all measurements, the antennas were in the LOS. The received signals were expected to contain direct and diffused components. Diffused components result from reflection, diffraction and scattering processes. These components tend to mix at the receiver and hence modifying the value of the received signal.

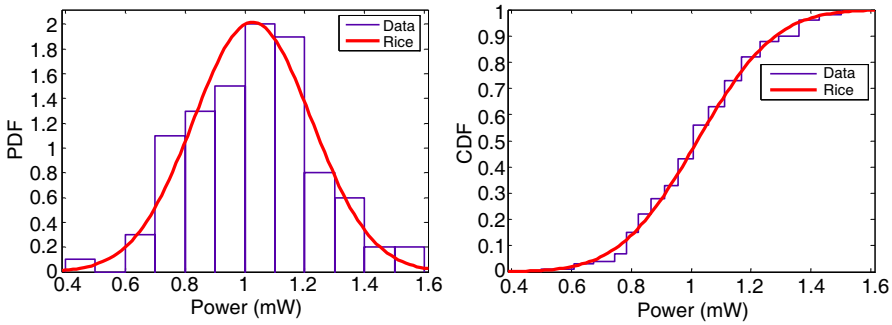

(a) (b)

Figure 8. Examples of probability distribution of small-scale signal variation, (a) PDF and (b) CDF.

From Equation (2), $p(x)$ is zero-mean in dBm. It was converted to $p(x')$ in milli-watts for evaluation using probability density functions. Figure 8 illustrates an example of Rice distribution fitting. A p-value of 0.05 has been used to accept or reject the null hypothesis in the goodness-of-fit test. In evaluating the distributions, Chi-square goodness of fit was used to rank the distribution. In some cases, Chi-square determines the null hypothesis to be true whilst K-S test rejects it. Examples of the probability density functions (PDF) assessed include the following:

$$P_{ri}\left(x'\right) = \frac{x'}{\sigma^2} e^{-\left[\frac{x'^2-\nu^2}{2\sigma^2}\right]} I_0\left(\frac{x'\nu}{\sigma^2}\right) \tag{8}$$

$$P_{na}\left(x'\right) = \frac{2m^m}{\Gamma(m)\Omega^m} x'^{2m-1} e^{-\frac{mx'^2}{\Omega}} \tag{9}$$

$$P_{ray}\left(x'\right) = \frac{x'}{\sigma^2} e^{-\frac{x'^2}{2\sigma^2}} \tag{10}$$

where $P_{ri}(x')$, $P_{na}(x')$, and $P_{ray}(x')$ are Rice, Nakagami and Rayleigh probability density functions (PDF), respectively; σ is the standard deviation of x'; ν is the amplitude of the LOS component, I_0 is the modified Bessel function of the first kind and zero order, Ω is the scale parameter equal to the mean value of x' and m is the Nakagami parameter [42, 43]. To analyse multipath fading effect, the Rice Factor, K, can be used. The Rice K-factor is the ratio of the direct and diffuse components as given by Equation (11).

$$K = \frac{\nu^2}{2\sigma^2} \tag{11}$$

where K is the Rice K-Factor, ν and σ are the same as in Equation (8) [39, 40].

In some cases, the Nakagami distribution fitted the data slightly better than Rice distribution, especially at low signal to noise ratio levels. However outage probabilities highly depend on the tail of the PDF for small power of the wanted signal. The probability of deep fades or small signals differs for Nakagami and Rice distributions, such that an approximation of the PDF of a Rician-fading wanted signal by a Nakagami PDF can be highly inaccurate [44].

Figure 9 shows examples of Rice K-factor variation with antenna separation. The figure shows that surface roughness has a significant influence on K-factor with smooth surfaces (sport court) having large values (up to 25 dB) and the grass field with the smallest values, less than 16 dB. A large K value indicates good propagation condition and it can be achieved either by strong direct component or weak

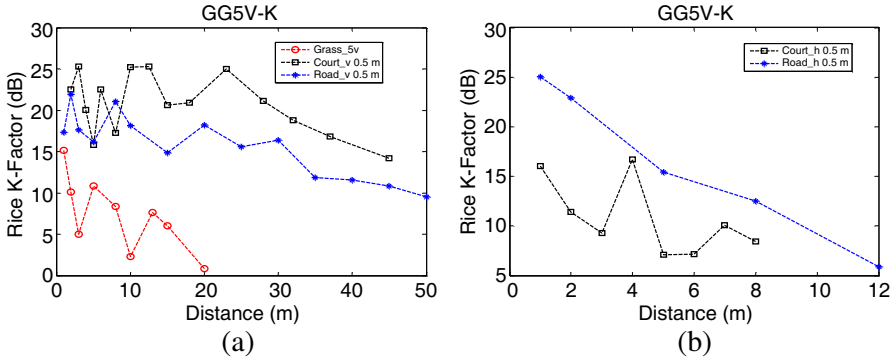

Figure 9. Rice K-Factor variation with distance at 0.5 m antenna height, (a) vertical and (b) horizontal, antenna orientation.

diffuse components in the received signal. The rate of change of K-factor with distance is also different for the different surfaces. The steepest gradient is obtained from the measurements in the grass field. Up to 8 m antenna separation on the road, the curve shows significant variations. This distance increases to 12 m on the grass and 20 m on the sport court. Over these distances, the received signal is dominated by strong coherent components where any reflected signal component has relatively large amplitude which would introduce significant multipath fading, depending on the relative time-delay with the direct component. Ground reflected paths will exist when the boundary of the first Fresnel Zone, h_0 is equal to or greater than, the antenna height [45].

$$h_0 = \frac{1}{2}\sqrt{\lambda d} \tag{12}$$

where d is the antenna separation and λ is the wavelength. At 2.4 GHz, $h_0 = 0.5$ m at 8 m which corresponds to the highest antenna height used in this study. Beyond 20 m for measurement on the grass, the variation of signal level is described by Nakagami distribution. At 2 m distance on the sport court and at antenna height of 0.5 m, the K-factor for vertical antenna orientation is 23 dB, Figure 9(a), but drops to 16 dB at the same distance for horizontal orientation, Figure 9(b). However on the road, the K-factors are similar at the same distance for both antenna orientations. The rough road surface is more effective in scattering the signal reducing the power of individual components but results in a large number of components that propagate in different directions. On the smooth sport court, fewer components with high amplitudes are reflected which when received, result in an overall smaller K-factor. At ground level, Rice K-factor decreases rapidly from

20 dB (court) and 18.5 dB (road) at 1 m distance to 6 dB and 2 dB at 8 m, respectively.

Since the signal variation about the mean at each position can be described by a statistical distribution, short path wireless sensor channel model on road surfaces and sports ground can be modeled using a combination of large- and small-scale fading. The analysis shows that Rice distribution can reliably be used to describe these channels for signal-to-noise ratios (SNR) greater than 10 dB. At smaller SNR the small-scale signal variation distribution is less certain and this study shows that it can be described by a number of distributions that include Nakagami, Rayleigh, Weibull and Normal distributions.

Since the vertical antenna position gives an optimum performance, it is used as the reference for low rate wireless personal area network planning. The first order model over estimates the maximum range at 0.5 m antenna height. Using the second order polynomial model and allowing a 5 dB margin for small-scale variation above the receiver sensitivity of −90 dBm, the maximum communication range is 60 m on the road and 70 m on the sport court.

5. CONCLUSIONS

This paper has presented WSN signal propagation in locations with three different surfaces: smooth hard sport court, tarred road and grass field. This study was conducted to provide the necessary knowledge for low data rate WSN deployments in these environments. A wide range of applications that would use these channels include road surface monitoring, curb to vehicle communications, application in sports for arena and athlete monitoring, vehicle guidance systems, structure monitoring, etc.. Robot localization based on signal propagation characteristics, especially in areas where global positioning system technology is not applicable, rely on a good understanding of signal propagation. Antenna misalignment or disorientation is also expected to be one characteristic of WSN deployment with node performances varying from worst case (complete misalignment or disorientation) to best case when fully aligned.

From the results, the best position for optimum performance in WSN propagation is vertical patch antenna orientation. The results have shown that the PER is less than 5.0% for received signal power within 5 dBm of the receiver sensitivity level of −90 dBm in an open unobstructed channel. However PER at low signal to noise ratios is very sensitive to channel variations and readily deteriorates to 100%. The average signal power and Rice K-factor decrease with distance. Rice K-factor exhibits significant variations at short path lengths

which can be attributed to strong multipath components from ground reflections. At large distances, multipath components are more diffused resulting in less fade depths and a steadier trend of K-factor variation with distance. Although the channel can be described as Ricean, at signal levels within 10 dBm of the receiver sensitivity, signal variation did not have a consistent distribution and Nakagami, Normal, Rayleigh and Weibull distributions were amongst the models that could be used.

Node placement at ground level (0.09 m above the surface) reduces the range by almost a factor of 2 compared to placement at 0.5 m. The same is true for horizontal positioning of the antenna at 0.5 m. Horizontal orientation of the antenna at ground level limits the transmission range to 5 m. Therefore, where unplanned ah-hoc node deployment is envisaged, node height above the surrounding grounds is more important than antenna orientation.

For all surfaces studied, maximum range is achieved on the hard sport court followed by on the road surface and then grass field. The major difference between the sport court and the road surface was the surface roughness with the sport court having a smoother surface. This means stronger and specula signal reflections which introduce significant frequency selective fading on the court. On the road surface more scattering occurred. Compared to other set-ups, a second order polynomial model was found to give a far better fit to measurements at 0.5 m vertical antenna orientation on the sport court and road than in other scenarios. The complexity of such higher order model was not justified for other cases because improvements in root mean square error was less than 0.3 dB compared to a first order model. Overall, the maximum optimum communication range for 0 dBm wireless sensor node transmission with a patch omni-directional antenna in the environments studied is 70 m.

ACKNOWLEDGMENT

The authors would like to express appreciation to Professor Syed Idris Syed Hasan and Mohd. Ezanuddin Abd. Aziz from Universiti Malaysia Perlis and Dr. Nor Idayu Mahat from Universiti Utara Malaysia for their assistance with the initial study. This research was funded by the Malaysian Ministry of Science, Technology and Innovation under e-Science Fund grant No. 03-01-15-SF0025.

REFERENCES

1. Eady, F., *Hands-on ZigBee Implementing 802.15.4 with Microcontrollers*, Elsevier Inc., Newnes, United Kingdom, 2007, ISBN:

0123708877.

2. Halgamuge, M. N., M. Zukerman, K. Ramamohanarao, and H. L. Vu, "An estimation of sensor energy consumption," *Progress In Electromagnetics Research B*, Vol. 12, 259–295, 2009.
3. Liu, H.-Q., H.-C. So, K. W. K. Lui, and F. K. W. Chan, "Sensor selection for target tracking in sensor networks," *Progress In Electromagnetics Research*, Vol. 95, 267–282, 2009.
4. Liu, H.-Q. and H.-C. So, "Target tracking with line-of-sight identification in sensor networks under unknown measurement noises," *Progress In Electromagnetics Research*, Vol. 97, 373–389, 2009.
5. Sim, Z. W., R. Shuttleworth, M. J. Alexander, and B. D. Grieve, "Compact patch antenna design for outdoor RF energy harvesting in wireless sensor networks," *Progress In Electromagnetics Research*, Vol. 105, 273–294, 2010.
6. Nadimi, E. S., H. T. Sogaard, and T. Bak, "ZigBee-based wireless sensor networks for classifying the behaviour of a herd of animals using classification trees," *Biosystems Engineering*, Vol. 100, 167–176, 2008.
7. Nadimi, E. S., H. T. Sogaard, T. Bak, and F. W. Oudshoorn, "ZigBee-based wireless sensor networks for monitoring animal presence and pasture time in a strip of new grass," *Computers and Electronics in Agriculture*, 1–9, 2007.
8. Lopez, M., S. Martinez, J. M. Gomez, A. Herms, L. Tort, J. Bausells, and A. Errachid, "Wireless monitoring of the pH, NH4+ and temperature in a fish farm," *Procedia Chemistry*, Vol. 1, 445–448, 2009.
9. Riquelme, J. A. L., F. Soto, J. Suardiaz, P. Sanchez, A. Iborra, and J. A. Vera, "Wireless sensor networks for precision horticulture in Southern Spain," *Computers and Electronics in Agriculture*, Vol. 68, 25–35, 2009.
10. Gay-Fernandez, J. A., M. Garcia Sanchez, I. Cuinas, A. V. Alejos, J. G. Sanchez, and J. L. Miranda-Sierra, "Propagation analysis and deployment of a wireless sensor network in a forest," *Progress In Electromagnetics Research*, Vol. 106, 121–145, 2010.
11. Mitilineos, S. A., D. M. Kyriazanos, O. E. Segou, J. N. Goufas, and S. C. A. Thomopoulos, "Indoor localisation with wireless sensor networks," *Progress In Electromagnetics Research*, Vol. 109, 441–474, 2010.
12. Verdone, R., D. Dardari, G. Mazzini, and A. Conti, *Wireless Sensor and Actuator Networks Technologies, Analysis and Design*,

Academic Press, Elsevier Inc., United Kingdom, 2008.

13. Chen, Y., Z. Zhang, L. Hu, and P. B. Rapajic, "Geomatry-based statistical model for radio propagation in rectangular office buildings," *Progress In Electromagnetics Research B*, Vol. 17, 187–212, 2009.
14. Chen, Y., Z. Zhang, and T. Qin, "Geomatrically based channel model for indoor radio propagation with directional antennas," *Progress In Electromagnetics Research B*, Vol. 20, 109–124, 2010.
15. Howitt, I. L. and M. S. Khan, "A mode based approach for characterizing RF propagation in conduits" *Progress In Electromagnetics Research B*, Vol. 20, 49–64, 2010.
16. Su, W. and M. Alzaghal, "Channel propagation characteristics of wireless MICAz sensor nodes," *Ad Hoc Networks*, 1–11, 2008.
17. Wyne, S., T. Santos, F. Tufvesson, and A. F. Molisch, "Channel measurements of an indoor office scenario for wireless sensor applications," *IEEE Global Communications Conf.*, 3831–3836, 2007.
18. Benkic, K., M. Malajner, P. Planinsic, and Z. Cucej, "Using RSSI value for distance estimation in wireless sensor networks based on ZigBee," *IEEE Inter. Conf. on Systems, Signals and Image Processing*, 303–306, 2008.
19. Xia, F., Y. C. Tian, Y. Li, and Y. Sun, "Wireless sensor/actuator network design for mobile control applications," *Sensors*, Vol. 7, 2157–2173, 2007.
20. Siden, J., A. Koptyug, M. Gulliksson, and H. E. Nilsson, "An action activated and self powered wireless forest fire detector," *International Federal for Information Processing 2007*, 47–58, 2007.
21. Phaebua, K., R. Suwalak, C. Phongcharoenpaniach, and M. Krairiksh, "Statistical characteristic measurements of propagation in durian orchard for sensor network at 5.8 GHz," *IEEE Inter. Symposium on Communications and Information Technology*, 520–523, 2008.
22. Kim, S., S. Pakzad, D. Culler, J. Demmel, G. Fenves, S. Glaser, and M. Turon, "Health monitoring of civil infrastructures using wireless sensor networks," *Proc. of 6th Inter. Conf. on Information Processing in Sensor Networks, IPSN'07*, 254–263, ACM Press, Cambridge, MA, Apr. 2007.
23. Anastasi, G., G. L. Re, and M. Ortolani, "WSNs for structural health monitoring of historical buildings," *Conference on Human System Interactions*, Catania, Italy, May 21–23, 2009.

24. Corredor, I., A. García, J. F. Martínez, and P. López, "Wireless sensor network-based system for measuring and monitoring road traffic," *6th CollECTeR Iberoamérica Conf.*, Madrid, Spain, Jun. 2008.
25. Iannizzotto, G., F. L. Rosa, and L. L. Bello, "A wireless sensor network for distributed autonomous traffic monitoring," *3rd Conference on Human System Interactions, HSI*, Rzeszow, Poland, May 2010.
26. Llosa, J., I. Vilajosana, X. Vilajosana, N. Navarro, E. Surinach, and J. M. Marques, "REMOTE, a wireless sensor network based system to monitor rowing performance," *Sensors*, Vol. 9, 7069–7082, 2009.
27. Dhamdhere, A., H. Chen, A. Kurusingal, V. Sivaraman, and A. Burdett, "Experiments with wireless sensor networks for real-time Athlete monitoring," *5th IEEE Inter. Workshop on Practical Issues in Building Sensor Network Applications, SenseApp 2010*, Denver, Colorado, USA, 2010.
28. Mottola, L., G. P. Picco, M. Ceriotti, S. Guna, and A. L. Murphy, "Not all wireless sensor networks are created equal: A comparative study on tunnels," *ACM Trans. on Sensor Networks*, Vol. 7, No. 2, Aug. 2010.
29. Shuai, M., K. Xie, X. Ma, and G. Song, "An on-road wireless sensor network approach for urban traffic state monitoring," *Proc. of 11th Int. IEEE Conf. on Intelligent Transportation Systems*, Beijing, China, Oct. 2008.
30. Megalingam, R. K., V. Mohan, M. Ajay, and P. L. S. Rizwin, "Wireless sensor network for vehicle speed monitoring and routing system," *IET Int. Conf. on Wireless Sensor Network*, Beijing, China, Nov. 2010.
31. Mouftah, H. T., M. Khanafer, and M. Guennoun, "Wireless sensor network architectures for intelligent vehicular systems," http://www.mcit.gov.sa/nr/rdonlyres/08880e2f-f4c9-4029-988f-05bf1379516d/0/paper2.pdf, accessed 14, Nov. 2011.
32. Franceschinis, M., L. Gioanola., M. Messere, R. Tomasi, M. A. Spirito, and P. Civera, "Wireless sensor networks for intelligent transportation systems," *IEEE Vehicular Technology Conf.*, Barcelona, Spain, Jun. 2009.
33. Ndzi, D. L., K. Stuart, S. Toautachone, B. Vuksanovic, and D. A. Sanders, "Wideband sounder for dynamic and static wireless channel characterisation: Urban picocell channel model," *Progress In Electromagnetics Research*, Vol. 113, 285–312, 2011.

34. MRF24J40MA Datasheet: 2.4 GHz IEEE Std. 802.15.4 RF Transceiver Module (DS70329A), Microchip Technology Inc., 2008.
35. Wireless Medium Access Control (MAC) and Physical Layer (PHY) Specifications for Low-Rate Wireless Personal Area Networks (LR-WPAN) Standard 2003, 14, IEEE Computer Society, 2003.
36. Myneni, S. and T. Manolescu, "MRF24J40 radio utility driver program, AN1192," *Microchip Tech. Inc.*, 2009.
37. Mahalin, N. H., H. S. Sharifah, S. K. S. Yusof, N. Fisal, and R. A. Rashid, "RSSI measurements for enabling IEEE 802.15.4 coexistence with IEEE 802.11 b/g," *TENCON 2009, IEEE Region 10 Conference*, 1–4, Singapore, 2009.
38. Petrova, M., R. Riihijarvi, P. Mahonen, and S. Labella, "Performance study of IEEE 802.15.4 using measurements and simulations," *IEEE Wireless Communications and Networking Conference, (WCNC 2006)*, 487–492, Las Vegas, NV, Apr. 2006.
39. Shankar, P. M., *Introduction to Wireless Systems*, John Wiley & Sons Inc., New York, 2002.
40. Dal Bello, J. C. R., G. L. Siqueira, and L. Bertoni, "Theoretical analysis and measurement results of vegetation effects on path loss for mobile cellular communication systems," *IEEE Transactions Vehicular Technology*, 1285–1293, 2000.
41. NIST/SEMATECH, Engineering Statistics Handbook, http://itl.nist.gov/div898/handbook/eda/section3/eda35g.htm, Accessed 3, Oct. 2011.
42. Dobkin, D. M., *RF Engineering for Wireless Networks, Hardware, Antennas and Propagation*, Elsevier Inc., Newnes, United Kingdom, 2005.
43. Barclay, L., *Propagation of Radiowaves*, 2nd Edition, The Institution of Electrical Engineers, London, 2003.
44. Linnartz, J.-P. M. G., "Wireless communication reference website," 1996–2004, http://wireless.per.nl/reference/chaptr03/ricenaka/ricenaka.htm, Accessed 3, Oct. 2011.
45. Meng, Y. S., Y. H. Lee, and B. C. Ng, "Path loss modeling for near-ground VHF radio-wave propagation throught forest with tree-canopy reflection effect," *Progress In Electromagnetics Research M*, Vol. 12, 131–141, 2010.